Nigerian Journal of Physics (NJP)
ISSN online: 3027-0936
ISSN print: 1595-0611
DOI: https://doi.org/10.62292/njp.v34i4.2025.198
Volume 34(4), December 2025

Upwelling Ion Observation from the Earth's Upper Atmosphere During EISCAT Svalbard Radar and FAST Satellite Conjunctions

*[1,2]Timothy W. David, [3]Emmanuel O. Adetunji, [2,4]Chizurumoke M. Michael, [2]Darren M. Wright, [1]Adetoro T. Talabi and [1]Abayomi E. Ajetunmobi

[1]Department of Physics, Olabisi Onabanjo University, Ago-Iwoye, Nigeria
[2]School of Physics and Astronomy, University of Leicester, Leicester, UK
[3]Department Basic Science, Babcock University, Ilishan, Nigeria
[4]Faculty of Art, Science and Technology, University of Northampton, Northampton, UK

*Corresponding author: Email: david.timothy@oouagoiwoye.edu.ng

ABSTRACT

The loss of planetary atmospheres is due to the process of heavy ions depletion from the upper atmosphere. It is a significant source of magnetospheric plasma and plays an important role in altering global magnetospheric dynamics. A number of mechanisms are responsible for these outflows, which include electron precipitation, joule heating and other suprathermal energization. Seven events are considered at a time that the Fast Auroral SnapshoT (FAST) satellite and EISCAT Svalbard radar (ESR) simultaneously detected ion upflow, and this is validated by ground-based radars called, the Cooperative UK Twin Located Auroral Sounding System (CUTLASS). ESR and CUTLASS observations around the time of conjunctions are analyzed. The results show that ESR observed upwelling ion flux to be ~ 10^{13} m^{-2} s^{-1}. Enhanced electron and ion temperatures are also observed at the time of these events. The dominant mechanism identified is the electron precipitation that results in an ambipolar electric field. The two striking events are the 2006-03-18 event that shows a distinct cusp signature indicated by CUTLASS and the 2002-01-20 event, which indicats a disturbed ionosphere due to data loss at ESR magnetic latitude.

Keywords:
Electron precipitation,
Ion upflow,
Ambipolar electric field,
Joule heating.

INTRODUCTION

Plasma originating from the ionosphere and entering the magnetosphere forms a substantial part of the plasma that populates the magnetosphere. The regions by which plasma from the ionosphere is energized into the magnetosphere are, the plasmasphere, auroral regions, and polar cap field-lines regions (Glocer *et al.,* 2009). Strangeway *et al.* (2005) stated that Alfvén speed slows down when mass from ionospheric outflows are added to flux tubes. This speed reduction thus affects the way in which the magnetosphere responds to changes in external drivers.

Dessler and Hanson in 1961 were the first to discuss the ionosphere as a source of magnetospheric plasma. They recognised that the terrestrial ionosphere is a significant potential source of plasma especially light ions, at high latitudes outside the plasmasphere. Schunk, (1999) and Albarran *et al.* (2024) extended this theme, exploring the formation of a steady polar ionosphere outflow into the magnetosphere (Moore *et. al*., 1999) and the references therein). Zhang and Brambles, (2021) and Hoffman *et al*. (1974) established by observation, the ionospheric supply of light ion plasma of polar wind outflow to the magnetosphere. The ionosphere supplies an amount of polar ion outflow that might be of sufficient strength to populate the earth's magnetosphere; both the quiet time light ion plasma and the heavy ion plasma characteristic of active times (Chappell *et al.,* 2000; Lin and Ilie, 2022). Former assumption was that the only notable ion outflow from the polar cap ionosphere was the polar wind that was first put forward by Axford in 1968. It was envisaged to be made up of light ions (H^+ and He^+) with few electron volts (Schunk, 2016). It was first observed that heavy ions of atmospheric source form a significant component of the magnetosphere through the composition measurement of Schunk, (2016). The measurements indicated a precipitation of energetic O^+ fluxes above that of H^+ at the time of geomagnetic storms. Since then, composition measurements on the Geostationary Operational Environmental Satellite

(GEOS) 1 and 2, Spacecraft Charging AT High Altitude (SCATHA), and International Sun-Earth Explorer (ISEE 1), in the high-altitude magnetosphere have shown significant availability of O^+ fluxes throughout the magnetosphere: in the ring current and the plasma sheet (Winglee *et al.,* 2005)

At thermospheric altitude, hydrogen experiences light gravitational attraction and as such, a slight rise in temperature releases substantial hydrogen atoms into the overlying space. The hydrogen density is thus increased above the thermosphere and decreased at lower altitudes of the thermosphere. According to Lin and Ilie (2022), the classical theory of plasma escape from the high-latitude ionosphere envisages that gravitational pull on heavy ions is strong while light ions (H^+ and He^+) require only the ambipolar electric field set up by ion-electron charge separation as a result of electron precipitation.

The heavy ion escape is dependent on geomagnetic storms and solar wind energy inputs, both in the form of photoionization of the Earth's neutral atmosphere by solar photons, and electromechanical energy (transmitted from the sun by the solar wind and linking the ionosphere through the magnetosphere) that heats the plasma (Lin and Ilie, 2022; Albarran *et al*., 2023). Moore *et al.* (1999) reported that the light ion polar wind is a pervasive feature of the polar regions and that these outflows fill the polar caps and lobes and continue into the near-Earth plasma sheet, in addition to the more energetic beams and conics of the auroral regions. These results suggest that the inner plasma sheet, and by extension the ring current plasma, may be dominantly supplied by ionospheric outflows. In contrast, solar plasma generally dominates the more distant boundary layers and plasma sheet.

Recent advances in understanding the geospace environment have made it increasingly clear that there is little about space weather that can be understood without reference to the ionosphere and magnetosphere.

The interconnectivity between the plasma of the ionosphere with that of the energetic and highly dynamical magnetosphere is the process known as magneto-ionospheric coupling. The process of interconnectivity is brought about by the Birkeland currents system, outflow mechanisms, wave heating, precipitating particles and electric fields (Figure 1).

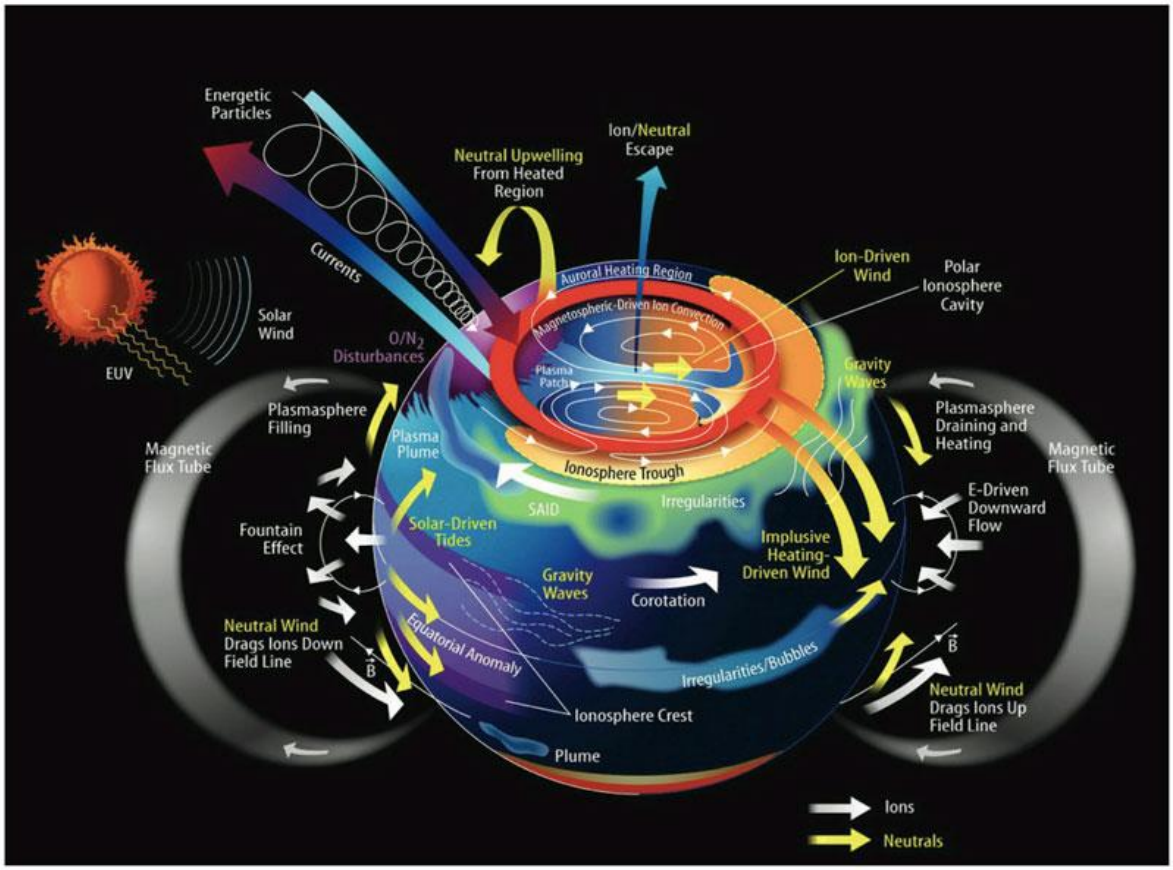

Figure 1: Magnetosphere-ionosphere coupling (http://esp.igpp.ucla.edu/research.html)

The ionosphere of the Earth and the magnetosphere combine to form a system of plasma, which provides all-encompassing in situ investigation and research. Its density scope between 10^{12} and 10^4 m^{-3} and temperature variation between 10^3 and 10^7 K has made it a valuable tool in the study of cosmic plasma. The local plasma is

even of more important because it is the scene of multiplex activities leading to particle energization and element separation. The comprehension of these activities is extremely important to stand in for distant astronomical spots, which could not be possible with in situ investigation. Planetary plasma has the capability for efficient particle acceleration, which occurs in the near-earth region, and this local plasma permits us to delineate the mechanisms that are accountable for it. The coupling between the magnetosphere and the ionosphere gives room for energy and momentum transfer between them (Tenfjord and Østgaard, 2013). There is a clear difference in the exchange, for instance, the chemical constituent of the plasma from the ionosphere to the magnetosphere is a singly ionized helium (He^{+}), while that from the solar source to the same sink is doubly ionized (alpha particle, He^{2+})

The complexity of the magneto-ionospheric coupling involves the electric field and mass movement. The movement can be from either the ionospheric region to the magnetosphere or vice versa. The flow from the magnetosphere, heating and auroral activity is brought about by the precipitation of high energy electron and proton. Indeed, ionospheric plasma is found in the magnetosphere during both quiet and active times (Glocer *et al.,* 2009).

The ionospheric plasma found in the magnetosphere can have a tremendous effect on the solution in the magnetosphere. Ionospheric outflows add mass to the magnetosphere, leading to:

i. decreased Alfvén speed on flux tubes
ii. reduced momentum/energy transfer rates
iii. a slower magnetospheric response time to external drivers
iv. changes in high-latitude magnetospheric dynamics
v. Magnetosphere-ionosphere coupling via Alfvén waves

Moreover, the presence of heavy ions can modify the ring current in the inner magnetosphere, impacting the D_{st} index and the local plasma beta.

The primary object of this study is to investigate the initial upwelling observations made by the ESR during outlows identified by the FAST satellite, and to validate these findings with another ground-based instrument - the CUTLASS radar. In comparison to previous works on upwelling ions (Endo *et al.,* 2000; Ogawa *et al.,* 2009; David *et al.,* 2018; David *et al.,* 2024, David *et al.,* 2025), where ion upflows where investigated based on meeting the ion velocity or ion flux threshold criteria, the presented work considers the study of upwelling that has already been observed by the FAST satellite to be leaving the Earth's auroral regions.

Instrumentation

FAST

Fast Auroral SnapshoT (FAST) satellite shown in Figure 2 is one of the Small Explorer (SMEX) missions by the National Aeronautics Space Agency (NASA), in fact, the second, in order to make a quick but detailed scientific observations at not very high cost (Harvey *et al*., 2001; Zhou *et al.,* 2003). The multiplex spacecraft was configured to take in situ measurements above the Earth's auroral regions. The FAST spacecraft measures the acceleration of particles and takes readings that would assist in the understanding of the auroral processes. It completes a revolution in about 2¼ hours, and with its apogee altitude of a little above 4000 km, it can venture high into the territory of the particles that create the aurora (Pfaff *et al.,* 2001; Ergun, 2001; Carlson *et al.,* 2001; Baddeley *et al.,* 2023). The FAST spacecraft was put into orbit on 21st August, 1996, at a respective apogee and perigee of 4175 km and 350 km by a rocket disengaged from a jet travelling at Mach 0.8. It carries instruments that carry out measurements above the Earth's auroral zones. The spacecraft has a tracking station monitored by NASA at Poker Flat, Alaska, collecting real-time data and another in Kiruna, Sweden, which is maintained by the European Space Agency (ESA) (Pfaff *et al.,* 2001; http://ham.space.umn.edu/spacephys/fast.html).

The spacecraft database has assisted scientists in reviewing theories about the nature of Earth's auroral. The FAST mission has helped in addressing key questions on the mechanisms responsible for particle acceleration, auroral formation, pitch-angle distribution of energetic auroral particles, and associated processes relating to the suprathermal energetic upflowing ions from the auroral ionosphere, which includes ion beams, ion conics and UWI (Carlson *et al.,* 1998; 2001; Pfaff *et al.,* 2001).

It is worthy to note that FAST's normal operations ended on May 1st, 2009, so, FAST is no longer gathering routine data (http://cse.ssl.berkeley.edu/fast_epo/).

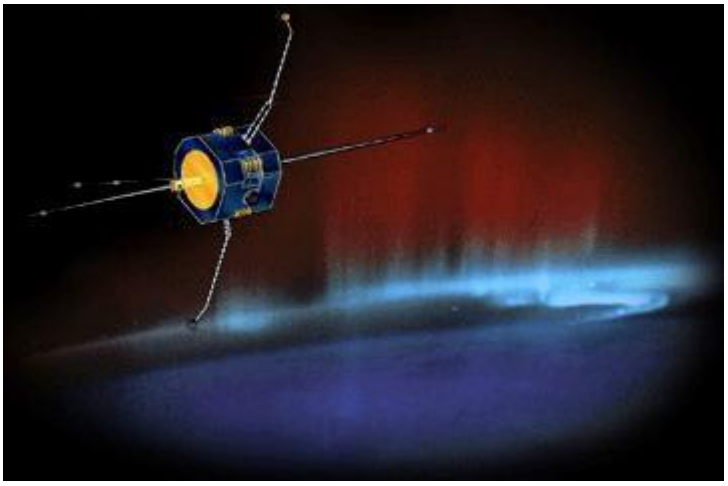

Figure 2: Fast Auroral SnapshoT (FAST) satellite
(source: Department of Physics, University of Leicester)

EISCAT

The EISCAT (European Incoherent Scatter) Scientific Association is a body set up to carry out research, using the ISR technique to probe the ionosphere as well as the different divisions (from lower to upper) of the atmosphere. EISCAT can also play the role of coherent scatter radar (CSR) in order to study ionospheric instabilities and investigate the dynamics of the middle atmosphere. Its heating facility could also be used to modulate the ionosphere for experimental purposes.

Ten ISRs are being operated in the world, of which EISCAT runs three of the highest-standard facilities. The present study is focused on the EISCAT Svalbard radar (ESR; Figure 3), situated close to Longyearbyen, Svalbard. The frequency of operation is in the 500 MHz band and it is being transmitted at a maximum power of 1.0 MW. In 1994, a facility credited for its very high gain and low noise performance, a fully steerable parabolic dish antenna of 32 m diameter was completed, and the ESR was officially launched on August 22, 1996 (Wannberg *et al.,* 1997). Also in 1999, another fixed field aligned antenna of 42 m diameter was added. The aim of locating this facility at high latitude is to foster, in particular, the studies of the cusp and polar cap region. (https://www.eiscat.se/about/whatiseiscat_new).

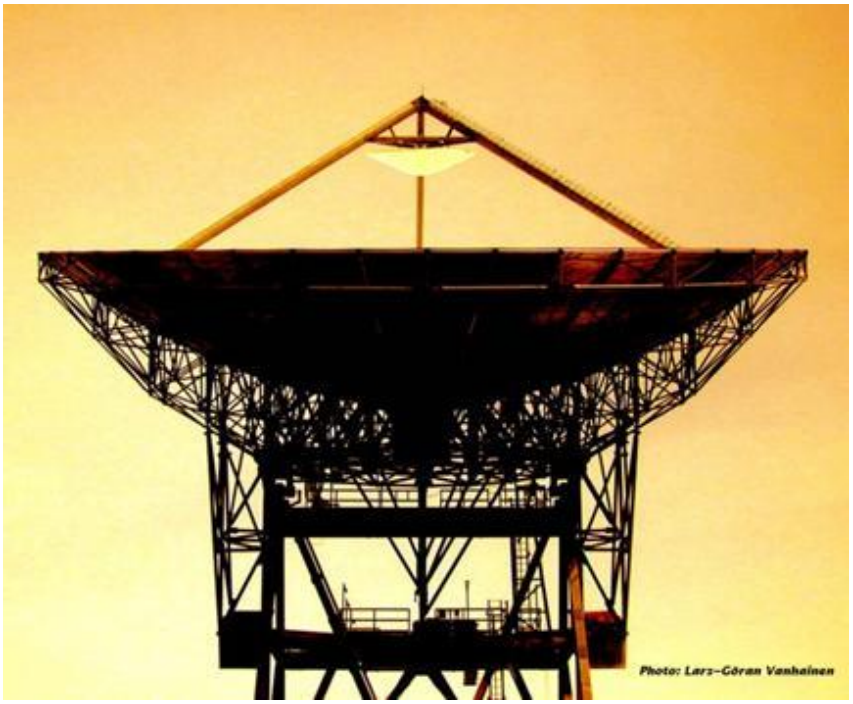

Figure 3: The EISCAT Svalbard Radar (http://www.eiscat.rl.ac.uk/)

SuperDARN

The Super Dual Auroral Radar Network (SuperDARN) is a worldwide chain of high frequency (HF) radars that monitor plasma dynamics in the high and middle latitude E and F regions of the ionosphere (Ribeiro *et al.,* 2013a; 2013b). The SuperDARN has been in operation since its inception over 20 years ago (Gillies *et al*., 2012), and it is a ground-based tool that has achieved considerable success in investigating both ionospheric and magnetospheric dynamics as well as the neutral atmosphere. The SuperDARN consists of several radars that employ the coherent-scatter radars (CSRs) technique operating in the HF band with a superposed fields-of-view that envelope the ionosphere above the hemispherical poles. The radar network has the principal objective of studying and measuring ionospheric convection, but has also achieved significant success at the magnetospheric altitudes (Chisham *et al*., 2007). The radars return measurements from plasma irregularities flowing up to several km s^{-1}, detectable to a range of thousands of kilometres, and by autocorrelation functions, the line-of-sight velocity, spectral width, and backscatter power can be estimated (Ribeiro *et al.,* 2013a; 2013b).

The CUTLASS radars

The two SuperDARN radars employed in this study are the bistatic pair of these radars called CUTLASS ('Cooperative UK Twin Located Auroral Sounding System'; Milan *et al.,* 1997). CUTLASS is a system that has agility for frequency, operating in the 8–20MHz bandwidth and comprises stations at Pykkvibær, Iceland, and the other pair at Hankasalmi, Finland (Wright *et al*., 2004; Millan *et al*., 1997). The CUTLASS radars consist of two arrays of log-periodic antennas, a main array of 16 antennas that can act both as transmitter and receiver, and an interferometer array of 4 antennas acting as a receiver only (Figure 4). The radars have fields of view enveloping a wide area, including the ESR facility (Figure 5), which is the area being considered under the present study (Millan *et al.,* 1997; Wright *et al.,* 2004). The northward-directed beam 9 of the Finland radar and beam 5 of the Iceland radar overlay the ESR facility (Millan *et al.,* 1997; Yeoman *et al.,* 2010), and are employed in this study as they pass through the coverage area of the EISCAT Svalbard Radar. The geographic co-ordinates of the Finland and Iceland radars are (62.32°N, 26.61°E) and (63.86°N, 19.20°W) respectively (Mark, 2013).

Figure 4: The CUTLASS radar

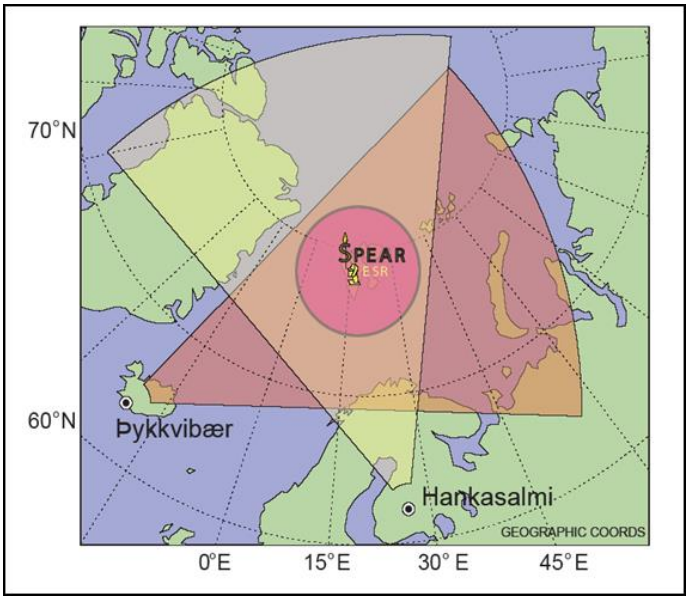

Figure 5: The CUTLASS radars fields-of-view in conjunction with ESR

Data and Analysis

This section examines data during conjunctions of the FAST spacecraft with the EISCAT ISRs and CUTLASS Coherent Scatter Radars (CSRs) at Longyearbyen, Svalbard. Over the whole lifetime of FAST (1996-2009), there were ~3000 conjunctions of FAST and ESR. Conjunctions between FAST and ESR considered so far were 283 intervals when ESR was operating, and only seven events were identified. The date, time, magnetic latitude, and other parameters during the conjunctions are presented in Table 1 below. Detailed analysis of two distinct events that met the threshold for ion upflow (David *et al.,* 2018; David *et al.,* 2024), a nightside event (2002-01-20) and one of the dayside events (2006-03-18) are presented in sections 4.1 and 4.2. The data used consist of the CUTLASS radar located at Hankasalmi, Finland, and the fixed field aligned antenna of 42 m diameter of the EISCAT Svalbard radar (ESR), available at the SuperDARN and Madrigal database, respectively.

Table 1: The date of events

FAST Orbit	Date	UT	Altitude (km)	MagLat (°)	GGLat (°)	GGLon (°)
5723	1998-02-01	11:30:34	3129	74.918	78.297	13.827
21560	2002-01-20	22:20:55	2666	74.673	78.607	19.691
36411	2005-09-12	11:25:01	3374	74.802	78.278	16.324
36478	2005-09-18	10:48:00	3104	74.643	78.172	16.64
38430	2006-03-11	09:21:54	3640	75.192	78.345	12.806
38508	2006-03-18	08:09:23	3728	74.111	77.78	20.058
46354	2008-02-14	12:07:05	1036	74.967	78.494	11.609

RESULTS AND DISCUSSION

Figures 6 and 7 present the power, line-of-sight velocity, and the spectral width from the SuperDARN parameter plot. Figures 8 and 9 show the electron density (N_e), electron temperature (T_e), ion temperature (T_i), ion velocity (V_i), and the ion flux (F_{ion}) from the ESR parameter plot. The black dotted lines in the figures indicate the conjunction time.

SuperDARN Parameter Plot

2002-01-20 event

The first event analyzed occurred around 22:21 UT, as presented in Figure 6. A few hours before the time of conjunction, the power plot shows high irregularities in the ionosphere throughout the time of investigation across the magnetic latitude as low as 65°. Though there was a paucity of data at the exact time of conjunction at the ESR magnetic latitude (MLAT 75.4°), which could be due to failure of the measuring instrument or a strong geomagnetic storm at that time, but data from the CUTLASS Finland radar indicate that strong flows toward the radar are present. It is worth noting that the second event on Table 1 is the only nightside event out of the seven conjunctions under study.

2006-03-18 event

Figure 7 presents the SuperDARN parameter plot between 06:10 UT and 10:00 UT for the March 18, 2006 event. The first panel shows a quite substantial disturbance in the ionospheric irregularities, which in turn gives rise to a high poleward flow speeds away from the radar as shown in the second panel. The line-of-sight velocity during the time of conjunction is above 800 m s^{-1} with a spectral width average of over 500 m s^{-1}. This indicates that data from the CUTLASS Finland radar signal strong cusp signatures during the dayside event.

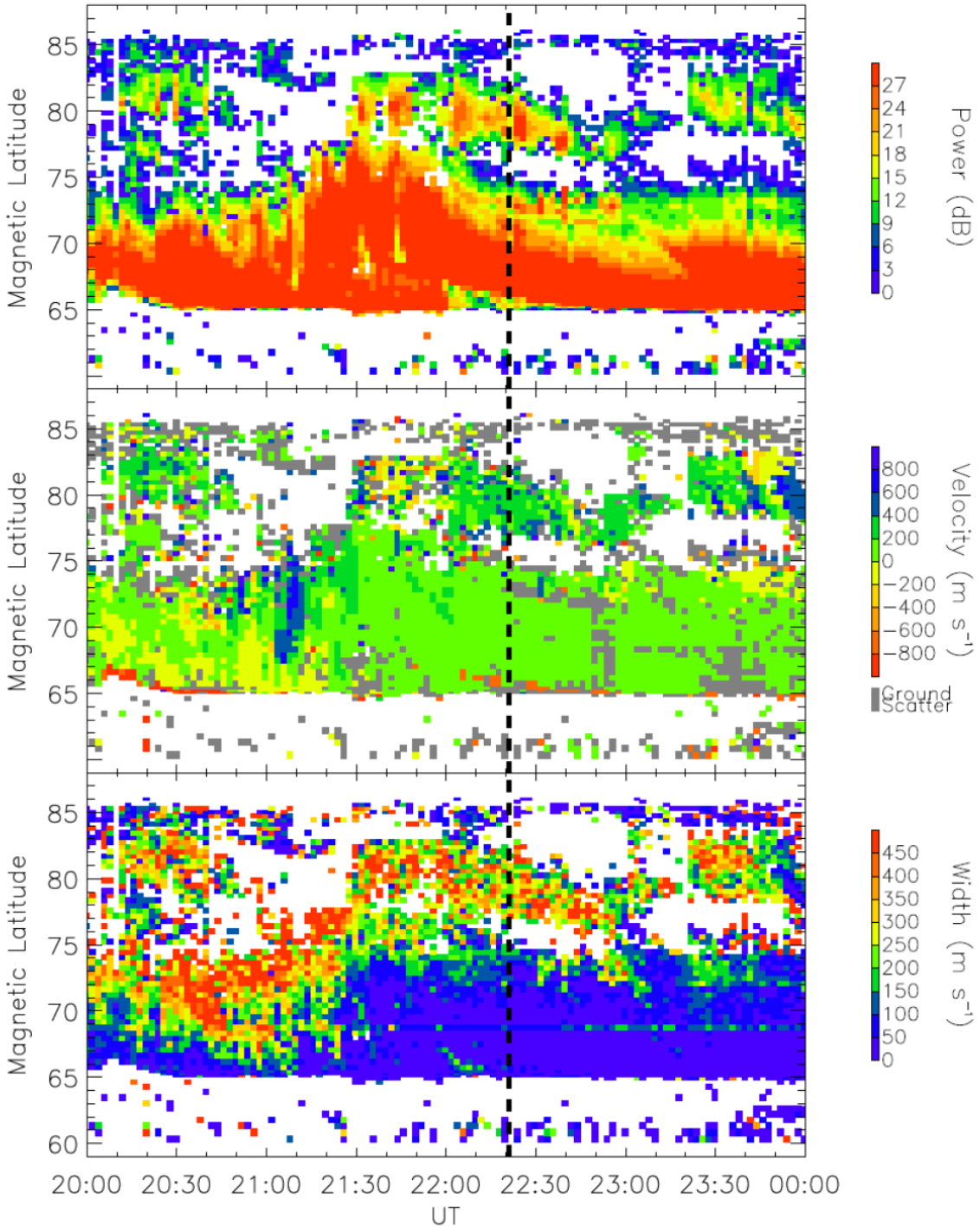

Figure 6: SuperDARN parameter plot for 2002-01-20 event: (a) power, (b) line-of-sight velocity, (c) spectral width

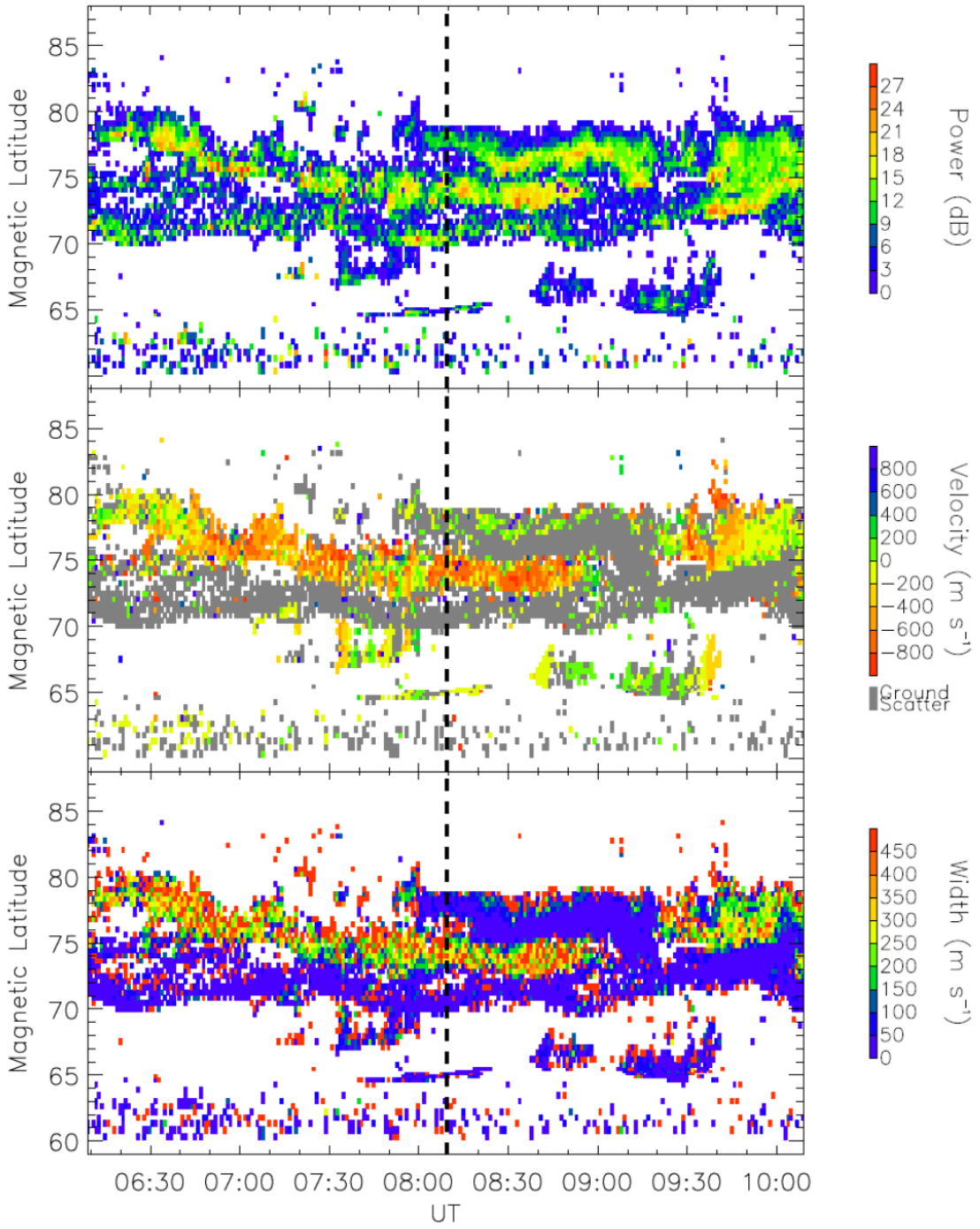

Figure 7: SuperDARN parameter plot for 2006-03-18 event: (a) power, (b) line-of-sight velocity, (c) spectral width

ESR Parameter Plot

Each of the plots in this section consists of five panels, which are electron density (N_e), electron temperature (T_e), ion temperature (T_i), ion velocity (V_i), and the ion flux (F_{ion}), respectively. The plots show variations in the above parameters with respect to altitude, ranging from 100 km to around 800 km. It is worth mentioning that positive values of velocity from the ESR data represent upward flow away from the radar.

2002-01-20 event

Figure 8 shows the January 20, 2002 event, which began with a stable electron density in the E-region from the period of 20:00 UT to around 21:30 UT. However, immediately after this time, strong electron precipitations

down to an altitude as low as the 100 km in the E-region dominate the rest of the period. The last panel in the figure shows that ESR observed enhanced ion flow between the interval 21:30 UT and 23:10 UT, which includes the time of conjunction at about 22:21 UT. Archer *et al.* (2015) had explained that the periods of elevated ion flow can lead to anisotropic ion temperature distribution, meaning that the ion is being heated preferentially in the direction perpendicular to the geomagnetic field compared to the parallel component of the ion temperature. Under such conditions and in the presence of the divergent geomagnetic field, the ions will experience an upward force, which Virtanen *et al.* (2014), called the hydrodynamic mirror force. It can be inferred from the works of Jones *et al.* (1988) and David *et al.* (2025) that in the presence of an anisotropic ion-velocity distribution function, which brings into play the magnetic mirror force, the conjunction of vertical upwelling of the neutral atmosphere and frictional heating of the ions will result in an adequate field-aligned velocity for the ions. The third and fourth panels in the figure show a good agreement with the existing theories.

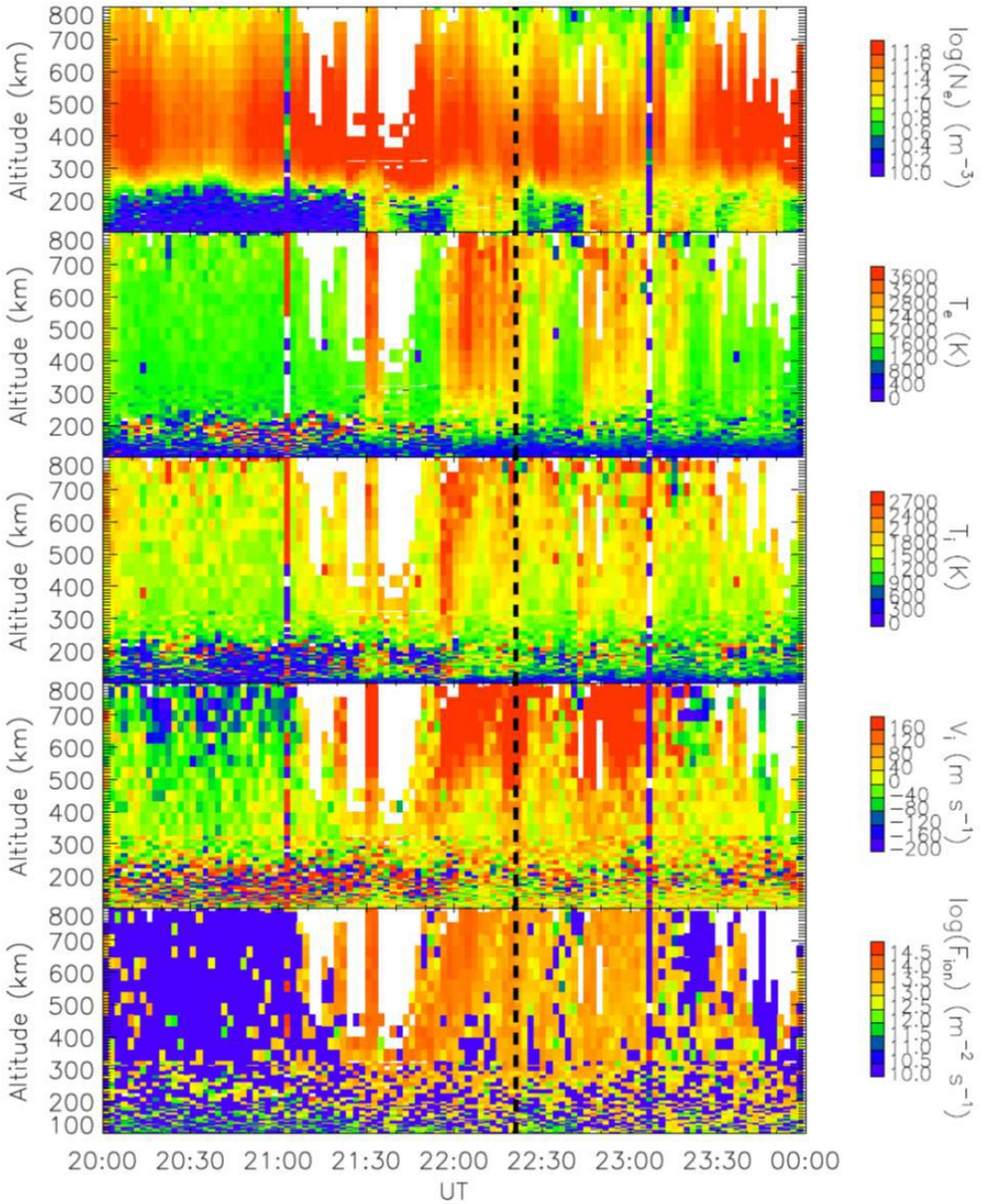

Figure 8: Ionospheric parameters observed by the EISCAT Svalbard Radar (ESR) on 2002-01-20: (a) electron density, (b) electron temperature, (c) ion temperature, (d) ion drift velocity, and (e) the ion flux

2006-03-18 event

Each of the five panels in Figure 9 indicates strong elevation of their respective characteristics at the conjunction time, around 08:09 UT. ESR data indicate strong precipitation immediately before the event and strong electron temperature almost throughout the period. At the conjunction time, the third panel shows a strong ion temperature elevation which becomes significantly enhanced through ion frictional heating, and this agrees with existing theory that there is a clear relationship between large ion velocities and ion temperature elevation (Goodwin *et al.,* 2018). The heating is most effective in the F-region altitude, modifying the plasma pressure gradient and resulting in field-aligned ion acceleration. A number of intervals of ion flow are evident in the figure, most obviously between 06:00 UT and 08:20 UT as well as 09:00 UT and 10:00 UT. However, the scales on this figure do not clearly indicate the magnitudes of the flow, but a more detailed investigation reveals that ion temperature above 5000 K and upward velocity of ~ 800 m s^{-1} occurred at the time of conjunction and at some other times. According to Wahlund and Opgenoorth (1989) and Wahlund *et al.* (1992) and Yau *et al*. (2011), the characteristics displayed by this event may classify it as a Type-II auroral bulk upflow.

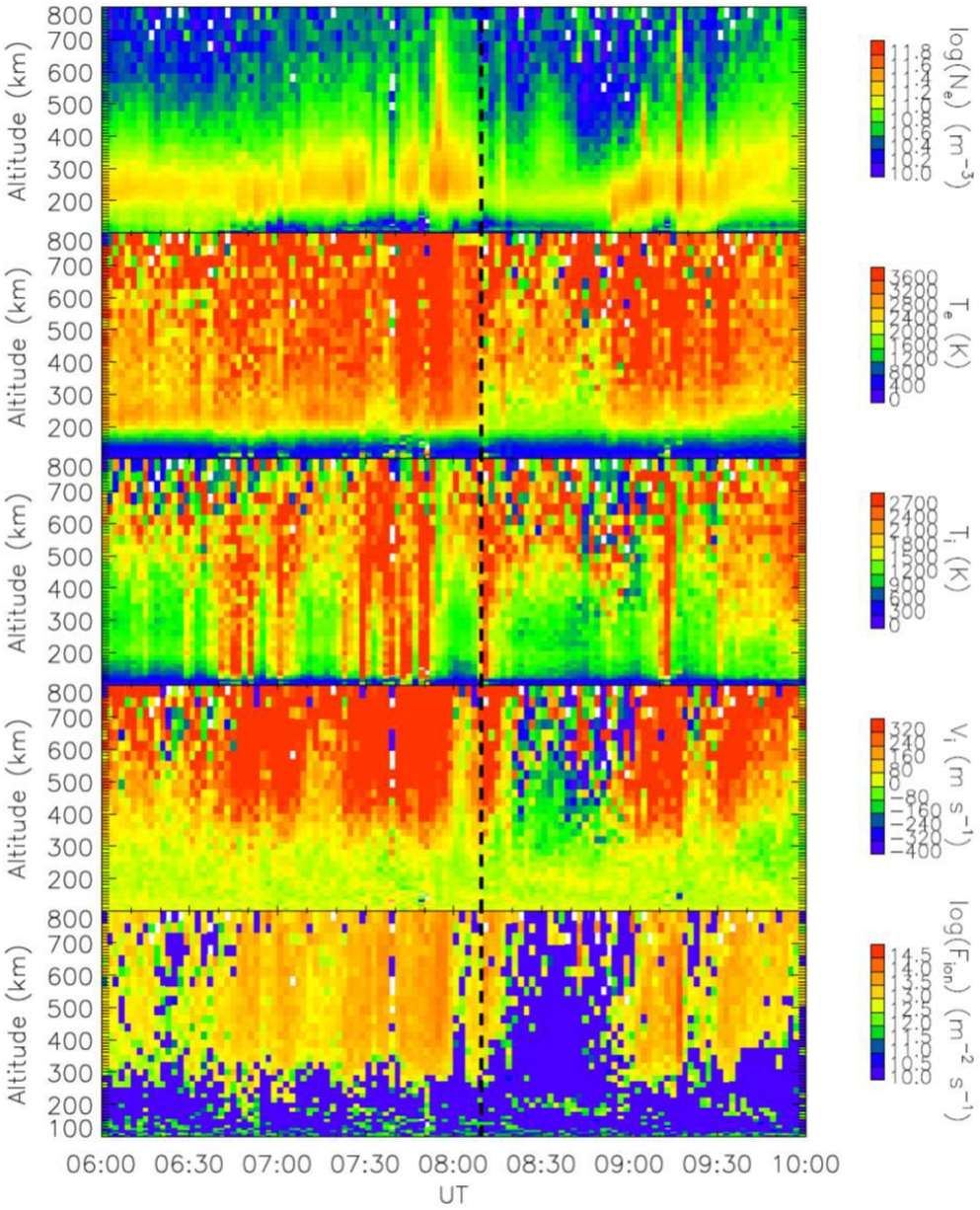

Figure 9: Ionospheric parameters observed by the EISCAT Svalbard Radar (ESR) on 2006-03-18: (a) electron density, (b) electron temperature, (c) ion temperature, (d) ion drift velocity, and (e) the ion flux

CONCLUSION

This study has investigated initial ion upflows from the Earth's upper atmosphere during seven conjunctions of the FAST spacecraft with the EISCAT Svalbard Radar (ESR), validated with ground-based CUTLASS SuperDARN radars. The analysis reveals that ESR consistently observed electron precipitation accompanied by enhanced electron and ion temperatures, with peak ion upflow fluxes on the order of ~10^{13} m^{-2} s^{-1} above 300 km altitude. Of the events analyzed, the 2006-03-18 dayside interval exhibited cusp signatures consistent with a Type-II auroral bulk upflow, while the 2002-01-20 nightside event demonstrated enhanced flows despite partial data loss, confirming the robustness of the upward flux signatures. These results demonstrate that electron precipitation–driven ambipolar electric fields and ion frictional heating are the dominant energization mechanisms during the observed events. The upwelling fluxes are of sufficient magnitude to make a non-negligible contribution to magnetospheric mass loading, thereby reducing Alfvén speeds along flux tubes and altering magnetosphere–ionosphere coupling on substorm and storm timescales. The presence of heavy ion outflows under both dayside cusp and nightside auroral conditions also highlights the variability of ionospheric contributions to the ring current and plasma sheet populations. By establishing quantitative benchmarks for ion upflow fluxes under conjunction conditions, this study provides observational evidence that supports theoretical models of ionospheric supply to the magnetosphere. Future coordinated analyses with multi-point satellite missions and next-generation ISR facilities will be necessary to resolve altitude-dependent energization processes, constrain uncertainties in flux magnitudes, and evaluate the cumulative role of upflow events in long-term magnetospheric dynamics.

REFERENCES

Albarran, R. M., Zettergren, M., Rowland, D., Klenzing, J., and Clemmons, J. (2023). Kinetic modeling of ionospheric outflows in pressure cooker environments. *Journal of Geophysical Research Space Physics*, *129* (1). https://doi.org/10.1029/2023ja031658

Albarran, R. M., Varney, R. H., Pham, K., and Lin, D. (2024). Characterization of N+ abundances in the terrestrial polar wind using the multiscale Atmosphere-Geospace environment. *Journal of Geophysical Research Space Physics*, *129*(5). https://doi.org/10.1029/2023ja032311

Archer, W. E., Knudsen, D. J., Burchill, J. K., Patrick, M. R., and St-Maurice, J. P. (2015). Anisotropic core ion temperatures associated with strong zonal flows and upflows. *Geophysical Research Letters*, *42*(4), 981–986. https://doi.org/10.1002/2014gl062695

Axford, W. I. (1968). The polar wind and the terrestrial helium budget. *Journal of Geophysical Research Atmospheres*, *73*(21), 6855–6859. https://doi.org/10.1029/ja073i021p06855

Baddeley, L., Lorentzen, D., Haaland, S., Heino, E., Mann, I., Miloch, W., Oksavik, K., Partamies, N., Spicher, A. and Vierinen, J., 2023. Space and atmospheric physics on Svalbard: a case for continued incoherent scatter radar measurements under the cusp and in the polar cap boundary region. *Progress in Earth and Planetary Science*, *10*(1), p.53.

Carlson, C. W., Pfaff, R. F., and Watzin, J. G. (1998). The Fast Auroral SnapShOT (FAST) mission. *Geophysical Research Letters*, *25*(12), 2013–2016. https://doi.org/10.1029/98gl01592

Carlson, C. W., McFadden, J. P., Turin, P., Curtis, D. W., and Magoncelli, A. (2001). The electron and ion plasma experiment for FAST. In *Springer eBooks* (pp. 33–66). https://doi.org/10.1007/978-94-010-0332-2_2

Chappell, C., Giles, B., Moore, T., Delcourt, D., Craven, P., and Chandler, M. (2000). The adequacy of the ionospheric source in supplying magnetospheric plasma. *Journal of Atmospheric and Solar-Terrestrial Physics*, *62*(6), 421–436. https://doi.org/10.1016/s1364-6826(00)00021-3

Chisham, G., Lester, M., Milan, S. E., Freeman, M. P., Bristow, W. A., Grocott, A., McWilliams, K. A., Ruohoniemi, J. M., Yeoman, T. K., Dyson, P. L., Greenwald, R. A., Kikuchi, T., Pinnock, M., Rash, J. P. S., Sato, N., Sofko, G. J., Villain, J., and Walker, A. D. M. (2007). A decade of the Super Dual Auroral Radar Network (SuperDARN): scientific achievements, new techniques and future directions. *Surveys in Geophysics*, *28*(1), 33–109. https://doi.org/10.1007/s10712-007-9017-8

David, T. W., Wright, D. M., Milan, S. E., Cowley, S. W. H., Davies, J. A., and McCrea, I. (2018). A Study of Observations of Ionospheric Upwelling Made by the EISCAT Svalbard Radar During the International Polar Year campaign of 2007. *Journal of Geophysical Research: Space Physics*, *123, 2192-2203,* https://doi.org/10.1002/2017JA024802

David, T. W., Michael, C. M., Wright, D., Talabi, A. T., and Ajetunmobi, A. E. (2024). Ionospheric upwelling and the level of associated noise at solar minimum. *Annales Geophysicae*, *42*(2), 349–354. https://doi.org/10.5194/angeo-42-349-2024

David, T. W., Michael, C. M., Wright, D. M., Talabi, A. T., Ajetunmobi, A. E., Awoyinka, T. D., and Kareem S. O. (2025). Case studies of drivers of ionospheric upwellings. *Indian Journal of Physics, 9*(2), 48–53, https://doi.org/10.1007/s12648-025-03582-4

Dessler, A.J. and Hanson, W.B. (1961). Possible energy source for the aurora. *Astrophysical journal,* 134, pp. 1024-1025

EISCAT Scientific Association, 01/13, 2014-last update, What is EISCAT. Available: https://www.eiscat.se/about/whatiseiscat_new [04/28, 2014].

Endo, M., Fujii, R., Ogawa, Y., Buchert, S. C., Nozawa, S., Watanabe, S., and Yoshida, N. (2000). Ion upflow and downflow at the topside ionosphere observed by the EISCAT VHF radar. *Annales Geophysicae*, 18(2), 170–181. https://doi.org/10.1007/s00585-000-0170-3

Foster, C., Lester, M., & Davies, J. A. (1998). A statistical study of diurnal, seasonal and solar cycle variations of F-region and topside auroral upflows observed by EISCAT between 1984 and 1996. *Annales Geophysicae*, 16(10), 1144–1158. https://doi.org/10.1007/s00585-998-1144-0

Ergun, R. E., Carlson, C. W., Mozer, F. S., Delory, G. T., Temerin, M., McFadden, J. P., Pankow, D., Abiad, R., Harvey, P., Wilkes, R., Primbsch, H., Elphic, R., Strangeway, R., Pfaff, R., and Cattell, C. A. (2001). The Fast Satellite Fields instrument. In *Springer eBooks* (pp. 67–91). https://doi.org/10.1007/978-94-010-0332-2_3

Gillies, R. G., Hussey, G. C., Sofko, G. J., and McWilliams, K. A. (2012). A statistical analysis of SuperDARN scattering volume electron densities and velocity corrections using a radar frequency shifting technique. *Journal of Geophysical Research Atmospheres*, *117*(A8). https://doi.org/10.1029/2012ja017866

Glocer, A., Tóth, G., Gombosi, T., and Welling, D. (2009). Modeling ionospheric outflows and their impact on the magnetosphere, initial results. *Journal of Geophysical Research Atmospheres*, *114*(A5). https://doi.org/10.1029/2009ja014053

Goodwin, L. V., St-Maurice, J., Akbari, H., and Spiteri, R. J. (2018). Incoherent scatter spectra based on Monte Carlo simulations of ion velocity distributions under strong ion frictional heating. *Radio Science*, *53*(3), 269–287. https://doi.org/10.1002/2017rs006468

Harvey, P. R., Curtis, D. W., Heetderks, H. D., Pankow, D., Rauch-Leiba, J. M., Wittenbrock, S. K., and McFadden, J. P. (2001). The FAST Spacecraft Instrument Data Processing Unit. In *Springer eBooks* (pp. 113–149). https://doi.org/10.1007/978-94-010-0332-2_5

Hoffman, J. H., Dodson, W. H., Lippincott, C. R., and Hammack, H. D. (1974). Initial ion composition results from the Isis 2 satellite. *Journal of Geophysical Research Atmospheres*, *79*(28), 4246–4251. https://doi.org/10.1029/ja079i028p04246

Hultqvist, B., Øieroset, M., Paschmann, G., & Treumann, R. A. (1999). Source processes in the high-latitude ionosphere. In *Space sciences series of ISSI* (pp. 7–84). https://doi.org/10.1007/978-94-011-4477-3_2

Jones, G. O. L., Williams, P. J. S., Winser, K. J., Lockwood, M., and Suvanto, K. (1988). Large plasma velocities along the magnetic field line in the auroral zone. *Nature*, *336*(6196), 231–232. https://doi.org/10.1038/336231a0

Lin, M. Y. and Ilie, R. (2022). A review of observations of molecular ions in the Earth's magnetosphere-ionosphere system. *Frontiers in Astronomy and Space Sciences*, *8*, p.745357

Mark, L. (2013). The Super Dual Auroral Radar Network (SuperDARN): An overview of its development and science. *ADVANCES IN POLAR SCIENCE*, *24*(1), 1-11. https://doi.org/10.3724/sp.j.1085.2013.00001

Milan, S. E., Yeoman, T. K., Lester, M., Thomas, E. C., & Jones, T. B. (1997). Initial backscatter occurrence statistics from the CUTLASS HF radars. *Annales Geophysicae*, *15*(6), 703–718. https://doi.org/10.1007/s00585-997-0703-0

Ogawa, Y., Buchert, S. C., Fujii, R., Nozawa, S., & van Eyken, A. P. (2009). Characteristics of ion upflow and downflow observed with the European Incoherent Scatter Svalbard radar. *Journal of Geophysical Research*, 114, A05305. https://doi.org/10.1029/2008JA013817

Pfaff, R., Carlson, C., Watzin, J., Everett, D., & Gruner, T. (2001). An overview of the Fast Auroral Snapshot (FAST) satellite. In *Springer eBooks* (pp. 1–32). https://doi.org/10.1007/978-94-010-0332-2_1

Ribeiro, A. J., Ponomarenko, P. V., Ruohoniemi, J. M., Baker, J. B. H., Clausen, L. B. N., Greenwald, R. A., and De Larquier, S. (2013). A realistic radar data simulator for the Super Dual Auroral Radar Network. *Radio Science*, *48*(3), 283–288. https://doi.org/10.1002/rds.20032

Ribeiro, A. J., Ruohoniemi, J. M., Ponomarenko, P. V., Clausen, L. B. N., Baker, J. B. H., Greenwald, R. A., Oksavik, K., and De Larquier, S. (2013). A comparison of SuperDARN ACF fitting methods. *Radio Science*, *48*(3), 274–282. https://doi.org/10.1002/rds.20031

Schunk, R. W. (2016). Polar Wind. In *Space Weather Fundamentals* (pp. 199-211). CRC Press.

Schunk, R. W. (1999). Ionospheric outflow. *Sun-Earth Plasma Connections*, *109,* 195-206.

STFC, Rutherford Appleton Laboratory, RAL Space, UK EISCAT support Group, 04/28, 2014-last update, support@eiscat.stp.rl.ac.uk. (n.d.). *UK EISCAT Support Group*. http://www.eiscat.rl.ac.uk/

Strangeway, R. J., Ergun, R. E., Su, Y., Carlson, C. W., and Elphic, R. C. (2005). Factors controlling ionospheric outflows as observed at intermediate altitudes. *Journal of Geophysical Research Atmospheres*, *110*(A3). https://doi.org/10.1029/2004ja010829

Tenfjord, P., and Ostgaard, N. (2013). Energy transfer and flow in the solar wind-magnetosphere-ionosphere system: A new coupling function. *Journal of Geophysical Research Space Physics*, *118*(9), 5659–5672. https://doi.org/10.1002/jgra.50545

University of California, B., 05/08, 2009-last update, FAST updates. Available: http://cse.ssl.berkeley.edu/fast_epo/ [28/04, 2014].

University of California, B., Los Angeles, Experimental Space Physics [Homepage of ULCA], [Online]. Available: http://esp.igpp.ucla.edu/research.html [05/16, 2014].

University of Minnesota, 09/04, 1998-last update, FAST. Available: http://ham.space.umn.edu/spacephys/fast.html [28/04, 2014].

Virtanen, I. I., McKay-Bukowski, D., Vierinen, J., Aikio, A., Fallows, R., and Roininen, L. (2014). Plasma parameter estimation from multistatic, multibeam incoherent scatter data. *Journal of Geophysical Research Space Physics*, *119*(12), 10,528 -10,543 https://doi.org/10.1002/2014ja020540

Wahlund, J., & Opgenoorth, H. J. (1989). EISCAT observations of strong ion outflows from the F-region ionosphere during auroral activity: Preliminary results. *Geophysical Research Letters*, *16*(7), 727–730. https://doi.org/10.1029/gl016i007p00727

Wahlund, J. -., Opgenoorth, H. J., Häggström, I., Winser, K. J., & Jones, G. O. L. (1992). EISCAT observations of topside ionospheric ion outflows during auroral activity: Revisited. *Journal of Geophysical Research Atmospheres*, *97*(A3), 3019–3037. https://doi.org/10.1029/91ja02438

Wannberg, G., Wolf, I., Vanhainen, L., Koskenniemi, K., Röttger, J., Postila, M., Markkanen, J., Jacobsen, R., Stenberg, A., Larsen, R., Eliassen, S., Heck, S., & Huuskonen, A. (1997). The EISCAT Svalbard radar: A case study in modern incoherent scatter radar system design. *Radio Science*, *32*(6), 2283–2307. https://doi.org/10.1029/97rs01803

Winglee, R. M., Lewis, W. and Lu, G. (2005). Mapping of the heavy ion outflows as seen by IMAGE and multifluid global modeling for the 17 April 2002 storm. *Journal of Geophysical Research: Space Physics*, *110*(A12), 1-15. https://doi.org/10.1029/2004JA010909

Wright, D. M., Yeoman, T. K., Baddeley, L. J., Davies, J. A., Dhillon, R. S., Lester, M., Milan, S. E., & Woodfield, E. E. (2003). High resolution observations of spectral width features associated with ULF wave signatures in artificial HF radar backscatter. *EGS - AGU - EUG Joint Assembly*, 3863. https://ui.adsabs.harvard.edu/abs/2003EAEJA.3863W/abstract

Yau, A. W., Peterson, W., and Abe, T. (2011). Influences of the ionosphere, thermosphere and magnetosphere on ion outflows. In *Springer eBooks* (pp. 283–314). https://doi.org/10.1007/978-94-007-0501-2_16

Yeoman, T. K., Klimushkin, D. Y., & Mager, P. N. (2010). Intermediate-m ULF waves generated by substorm injection: a case study. *Annales Geophysicae*, *28*(8), 1499–1509. https://doi.org/10.5194/angeo-28-1499-2010

Zhang, B. and Brambles, O. J., (2021). Polar Cap O+ Ion Outflow and Its Impact on Magnetospheric Dynamics. *Ionosphere Dynamics and Applications*, pp.83-114.

Zhou, X., Tsurutani, B. T., Reeves, G., Rostoker, G., Sun, W., Ruohoniemi, J. M., Kamide, Y., Lui, A. T. Y., Parks, G. K., Gonzalez, W. D., and Arballo, J. K. (2003). Ring current intensification and convection-driven negative bays: Multisatellite studies. *Journal of Geophysical Research Atmospheres*, *108*(A11). https://doi.org/10.1029/2003ja009881